Biochemistry

Article

pubs.acs.org/biochemistry

A Lysine-Targeted Affinity Label for Serine-β-Lactamase Also Covalently Modifies New Delhi Metallo-β-lactamase-1 (NDM-1)

Pei W. Thomas,[†] Michael Cammarata,[‡] Jennifer S. Brodbelt,[‡] Arthur F. Monzingo,[§] R. F. Pratt,*[,∥] and Walter Fast*[,†]

[†]Division of Chemical Biology and Medicinal Chemistry, College of Pharmacy, and LaMontagne Center for Infectious Disease, [‡]Department of Chemistry, and [§]Center for Biomedical Research Support, The University of Texas, Austin, Texas 78712, United States

[∥]Department of Chemistry, Wesleyan University, Middletown, Connecticut 06459, United States

ABSTRACT: The divergent sequences, protein structures, and catalytic mechanisms of serine- and metallo-β-lactamases hamper the development of wide-spectrum β-lactamase inhibitors that can block both types of enzymes. The *O*-aryloxycarbonyl hydroxamate inactivators of *Enterobacter cloacae* P99 class C serine-β-lactamase are unusual covalent inhibitors in that they target both active-site Ser and Lys residues, resulting in a cross-link consisting of only two atoms. Many clinically relevant metallo-β-lactamases have an analogous active-site Lys residue used to bind β-lactam substrates, suggesting a common site to target with covalent inhibitors. Here, we demonstrate that an *O*-aryloxycarbonyl hydroxamate inactivator of serine-β-lactamases can also serve as a classical affinity label for New Delhi metallo-β-lactamase-1 (NDM-1). Rapid dilution assays, site-directed mutagenesis, and global kinetic fitting are used to map covalent modification at Lys211 and determine K_I (140 μM) and k_{inact} (0.045 min^{-1}) values. Mass spectrometry of the intact protein and the use of ultraviolet photodissociation for extensive fragmentation confirm stoichiometric covalent labeling that occurs specifically at Lys211. A 2.0 Å resolution X-ray crystal structure of inactivated NDM-1 reveals that the covalent adduct is bound at the substrate-binding site but is not directly coordinated to the active-site zinc cluster. These results indicate that Lys-targeted affinity labels might be a successful strategy for developing compounds that can inactivate both serine- and metallo-β-lactamases.

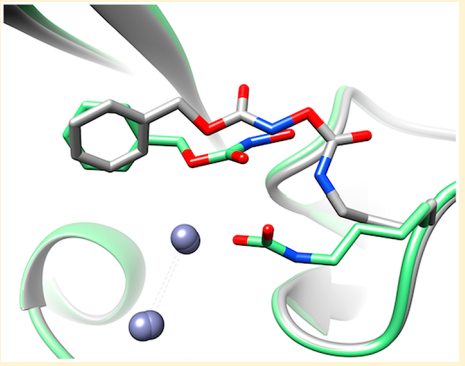

β-Lactam drugs comprise a large proportion of therapeutics regularly used to treat bacterial infections, but their usefulness is threatened by the emergence of resistant bacteria that often produce β-lactamase enzymes that degrade these drugs.[1] Co-treatment with β-lactamase inhibitors can effectively extend the lifetime and usefulness of β-lactam drugs. However, one of the challenges in designing wide-spectrum β-lactamase inhibitors is the different catalytic mechanisms used by metallo-β-lactamases and serine-β-lactamases. Clinically used β-lactamase inhibitor co-drugs such as avibactam work by mimicking the normal substrate and stabilizing a covalent reaction intermediate formed at the active-site Ser of serine-β-lactamases.[2] Therefore, these co-drugs cannot effectively inhibit metallo-β-lactamases that instead use a hydroxide nucleophile that is bound noncovalently at a dinuclear zinc ion site between zinc-1 (ligated by three His residues) and zinc-2 (ligated by Cys, His, and Asp residues) (Figure 1).[3,4]

Pratt and co-workers previously described a novel type of covalent inhibitor for serine-β-lactamases that possibly represents an alternative strategy (Figure 1a).[5−9] These *O*-aryloxycarbonyl hydroxamates (e.g., **1**), originally designed to mimic β-lactamase substrates, react covalently with the active-site Ser of serine-β-lactamases (**2**), as do typical substrates. However, after the initial covalent adduct is formed, the same carbonyl carbon that was first attacked by the active-site Ser is subsequently attacked by a neighboring Lys, which otherwise serves as a binding partner for the carboxylate of β-lactam substrates.[5,10] The resulting product left behind (**4**) consists of only two atoms, a single carbonyl group, that covalently cross-links two active-site residues, thereby abrogating activity.[5] Although metallo-β-lactamases lack a nucleophilic Ser, many contain an analogous Lys residue that helps zinc-2 anchor the carboxylate of β-lactam substrates (Figure 1b).[11] Because the *O*-aryloxycarbonyl hydroxamates were designed as substrate mimics, because they can target other β-lactam-binding enzymes, including the serine-β-lactamases TEM-2 and OXA-1, the R39 DD-peptidase from *Actinomadura*, and pencillin acylase, and because many metallo-β-lactamases share an analogous Lys residue that serves the same binding function, we hypothesized that the same affinity label designed for serine-β-lactamases might also work with metallo-β-lactamases.[6,12] Here, we show that *N*-(benzyloxycarbonyl)-*O*-[(phenoxycarbonyl)]hydroxylamine (**1**) also acts as a classical affinity label of New Delhi metallo-β-lactamase-1 (NDM-1)

Received: May 1, 2019
Revised: May 28, 2019
Published: May 30, 2019

DOI: 10.1021/acs.biochem.9b00393
Biochemistry XXXX, XXX, XXX−XXX

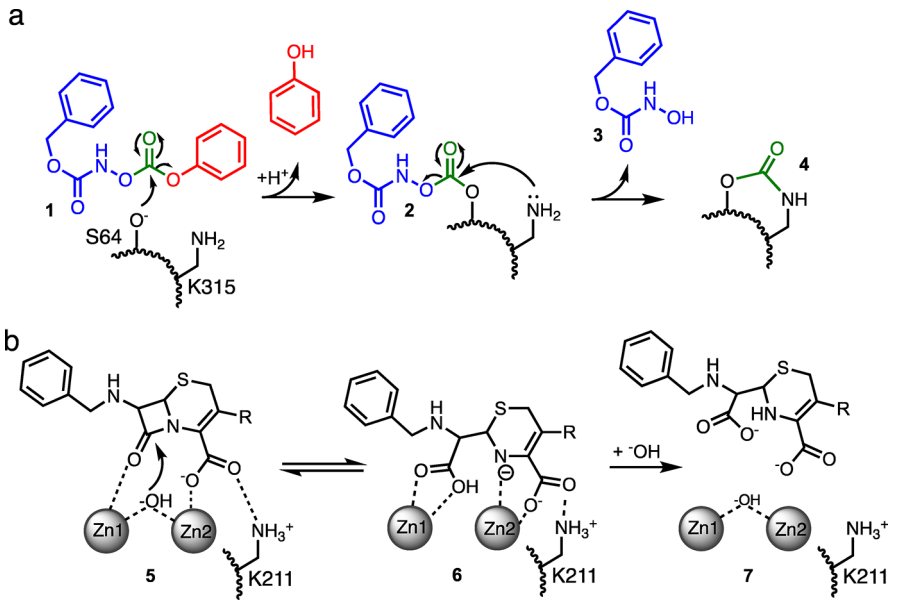

Figure 1. Proposed mechanisms of inactivation and turnover. (a) Proposed mechanism for inactivation of AmpC β-lactamase by an *O*-aryloxycarbonyl hydroxamate (**1**), with the phenol leaving group colored red, the hydroxamate "arm" colored blue (**3**), and the cross-linking carbonyl colored green (**4**). (b) Proposed mechanism of chromacef turnover by NDM-1, showing the Michaelis complex (**5**), the anionic intermediate (**6**), and the product complex (**7**), all noncovalently bound near zinc-1 (Zn1) and zinc-2 (Zn2) of the active-site dinuclear zinc cluster. Each enzyme has a Lys residue (a, K315; b, K211) that serves a similar function in binding β-lactam substrates.

and specifically targets the active-site Lys211 for covalent modification. Although further optimization will be required, this example serves as a proof of principle that Lys-targeted affinity labels can be used to target both mechanistically distinct classes of serine- and metallo-β-lactamase enzymes.

EXPERIMENTAL PROCEDURES

Purified NDM-1. For the experiments described below, a purified NDM-1 truncation missing the initial 35 amino acids was used, as described previously.[13] This truncation corresponds to the most predominant soluble fragment found in overexpression cultures of full-length NDM-1 and removes the site of posttranslational lipid modification that otherwise leads to membrane association.

Time-Dependent Inactivation of NDM-1 and NDM Variants. To monitor time- and concentration-dependent inactivation of NDM-1, we preincubated NDM-1 (2 μM) with various concentrations of **1** (0−2.0 mM). Stock solutions of **1**[5] (40 mM) were prepared in dry acetonitrile (ACROS organic), with a final co-solvent concentration in preincubation and assay solutions of 5% (v/v). At increasing time points, aliquots of the preincubation mixture were rapidly diluted (100-fold) into saturating amounts of the competing substrate for subsequent determination of the remaining enzyme activity by determining initial rates. The conditions and procedures used were the same as those described previously (50 mM HEPES, pH 7.0, 25 °C),[14] except that we added 0.02% Tween 20 and substituted chromacef[15] (20 μM, a generous gift from L. Sutton, Benedictine College, Atchison, KS) in place of nitrocefin as the reporter substrate, using a $\Delta\varepsilon_{442}$ of 14500 M^{-1} cm^{-1} as described previously.[16] The purified NDM-1 and its C208D and K211A variants were described previously.[14,17] To compensate for differences in k_{cat} and K_M values and zinc affinity among NDM-1 mutants, different concentrations of C208D NDM-1 (15 μM; this mutant has k_{cat} and K_M values lower than those of the wild type and binds zinc-2 more weakly) and K211A NDM-1 (0.2 μM; this mutant has k_{cat} and K_M values higher than those of the wild type) were used in the preincubation mixtures, and the concentrations of $ZnSO_4$ (10 μM) and inhibitor (1 mM) were increased in comparison to those in similar experiments using wild-type NDM-1.

Test for Inactivation by Product. To test whether a reaction product of NDM-1 and **1** was responsible for the observed inactivation, we used the procedure described above to monitor inactivation of NDM-1 (2 μM) by **1** (500 μM) during a 90 min incubation, and then a second aliquot (1 μL) of a fresh stock of uninhibited NDM-1 (1 mM, ~2 μM final concentration added) was added and the rapid dilution assay continued for an additional 60 min.

Non-Enzymatic Hydrolysis of 1. Under the conditions used for enzyme labeling, **1** undergoes non-enzymatic hydrolysis to release phenol.[5] The largest absorbance difference between **1** and phenol stock solutions occurs at 278 nm, so we used dilutions of a phenol standard solution (Ricca Chemical Co., Arlington, TX) to construct a linear standard curve that relates absorption at 278 nm to phenol concentration in the same buffer solution used for enzyme inactivation. A time-dependent increase in absorbance at 278 nm was then monitored upon dilution of **1** (0.4 mM) in assay buffer in the absence of enzyme, and the standard curve used to convert the change in absorption into a graph depicting phenol formation over time.

Global Kinetic Fitting. Data for non-enzymatic **1** hydrolysis and the time- and concentration-dependent inactivation of NDM-1 by **1** were loaded into KinTek Global Kinetic Explorer version 8 (Kintek Co., Snow Shoe, PA).[18,19] A kinetic model was entered to describe the non-enzymatic decay of **1** to an inactive product, as well as a two-step mechanism for inactivation of NDM-1 that includes an initial reversible binding step, followed by an irreversible inactivation. The on rate for binding was fixed at a typical diffusion-controlled rate (10^9 M^{-1} s^{-1}); the off rate and inactivation rates were kept

DOI: 10.1021/acs.biochem.9b00393
Biochemistry XXXX, XXX, XXX−XXX

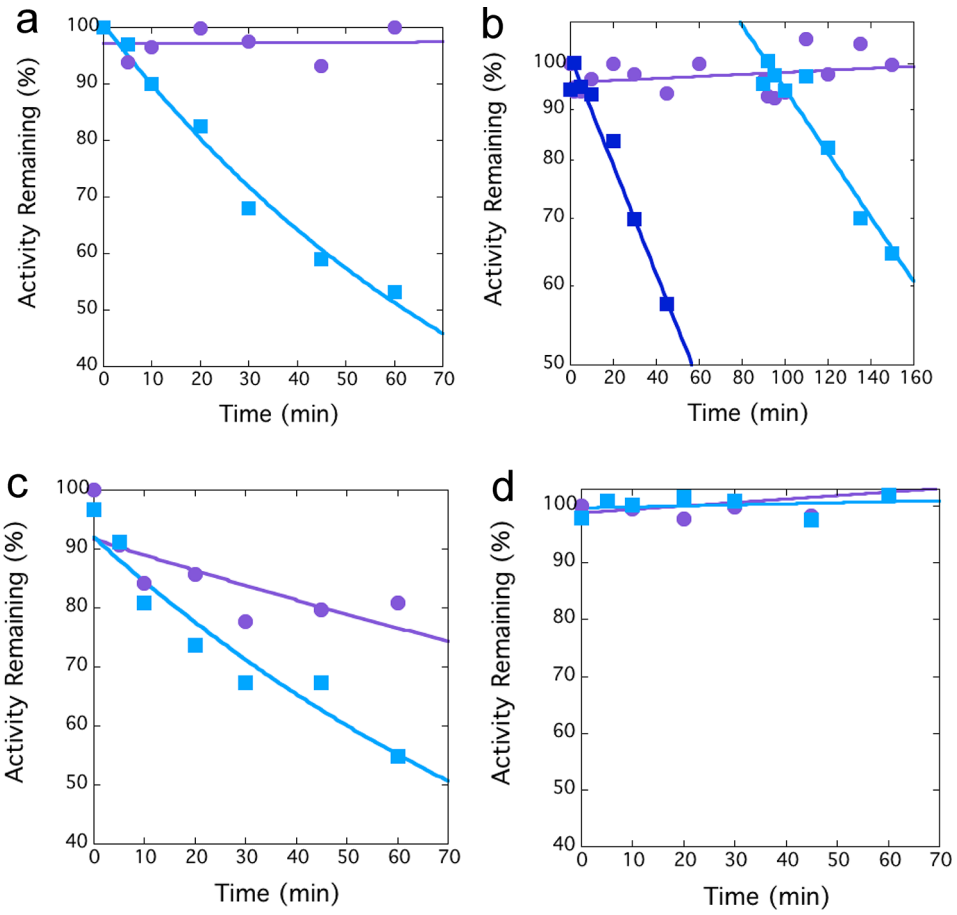

Figure 2. Time-dependent inactivation of NDM variants. (a) Dilution assays indicate time-dependent irreversible inactivation of NDM-1 by **1** (light blue squares, 10 μM), in contrast to a control incubation without the inactivator (purple circles). (b) Inactivation of NDM-1 by **1** (dark blue squares, 10 μM) is followed by addition of a second aliquot of the fresh enzyme to the same preincubation tube (light blue squares), with the activity immediately after addition reset to 100%. A control incubation did not include the inactivator (purple circles). (c) Dilution assays indicate time-dependent irreversible inactivation of C208D NDM-1 by **1** (light blue squares, 10 μM). The control incubation without the inactivator (purple circles) indicates the stability of the C208D NDM-1 variant is lower than that of wild-type NDM-1. (d) Dilution assays indicate no time-dependent irreversible inactivation of K211A NDM-1 by **1** (light blue squares, 10 μM), in comparison to a control incubation without the inactivator (purple circles). Fitting errors from incubations that showed appreciable inactivation were <15%.

variable, and the other experimental values (see above) were entered as starting conditions. The non-enzymatic decay rate constant, the rate constant for **1** dissociation, and the NDM-1 inactivation rate constant were then determined by global fitting and reported with the standard errors given by Global Kinetic Explorer for the best fits.

Mass Spectrometry. NDM-1 (16 μM) was incubated with **1** (2 mM) for 20 h in HEPES buffer (50 mM, pH 7.0). An untreated NDM-1 solution was used as a control. Prior to MS analysis, a centrifugal 10 kDa molecular weight cutoff filter was used to exchange buffer for water and to concentrate each protein solution. The samples were diluted to make ~15 μM protein solutions in a 59.25:39.25:0.5 (v/v/v) acetonitrile/water/formic acid mixture. The solutions were then infused into a Thermo Fisher Scientific Elite Orbitrap Mass Spectrometer equipped with a Coherent (Santa Clara, CA) ExciStar ArF (193 nm, 500 Hz pulse rate) excimer laser at a rate of 1.20 μL/min with a spray voltage of 3.5 kV. MS1 spectra for intact proteins were collected at 120000 resolution at m/z 400. The +28 charge state of NDM-1 inactivated by **1** was selected for ultraviolet photodissociation (UVPD) and activated using a single 2.0 mJ laser pulse. UVPD was performed in the higher-collision energy dissociation (HCD) cell located at the back end of the Orbitrap mass spectrometer as described previously,[20] with the pressure adjusted to 5 mTorr in the HCD cell. The resulting MS/MS spectra from UVPD were collected at 240000 resolution at m/z 400 and averaged for 1000 scans. Both the ESI mass spectra and the UVPD MS/MS spectra were deconvoluted using Xtract (Thermo Fisher Scientific) with a signal-to-noise cutoff of 2. MS/MS fragments were assigned using a modified version of ProSightPC to accommodate UVPD fragment ions with a fragment mass tolerance of 10 ppm.

Crystallization of 1-Treated NDM-1. Purified NDM-1 (12 mg/mL, with the initial 35 residues truncated) was preincubated with **1**. Crystals of the resulting complex were grown at room temperature by vapor diffusion using the sitting drop method from 0.2 M calcium chloride dihydrate and 20% polyethylene glycol (PEG) 3350.

X-ray Data Collection and Processing. A crystal resulting from **1**-treated NDM-1 was removed from its drop using a nylon loop and flash-frozen in liquid nitrogen. Diffraction data were collected at 100 K at Advanced Light Source beamline 5.0.3 at the Lawrence Berkeley National Laboratory with the assistance of the Berkeley Center for Structural Biology. Data were processed using HKL2000.[21]

DOI: 10.1021/acs.biochem.9b00393
Biochemistry XXXX, XXX, XXX−XXX

Structure Determination. Cell parameters of the crystal described above suggested that the asymmetric unit might contain two protein molecules. The solution of two NDM-1 molecules (each lacking the initial 35 residues) in the asymmetric unit was determined by molecular replacement with Phaser[22] using the structure of NDM1 with the initial 46 residues truncated[23] [Protein Data Bank (PDB) entry 3S0Z] as the search model.

Model building was carried out using Coot.[24] Refinement of models was done using PHENIX.[25] There were several rounds of refinement followed by manual rebuilding of the model. To facilitate manual rebuilding, difference maps and a $2F_o - F_c$ map, σA-weighted to eliminate bias from the model,[26] were prepared. A portion (5%) of the diffraction data was set aside throughout refinement for cross-validation.[27] MolProbity[28] was used to determine areas of poor geometry and to make Ramachandran plots. The final model does not include side chain atoms for which there was no observed electron density. Coordinates and structure factors were deposited in the PDB (entry 6OVZ).

RESULTS AND DISCUSSION

Affinity Labeling of NDM-1 by 1. To test for affinity labeling, we first incubated NDM-1 with an excess of **1**, removed aliquots at successive time points, and diluted each into saturating amounts of the excess substrate to test for remaining activity. The substrate is expected to outcompete any inhibitor that is bound noncovalently to the active site and result in fully recovered activity. However, covalent labeling is expected to be irreversible and result in a time-dependent loss of activity. **1** causes a time-dependent loss of NDM-1 activity that is irreversible to dilution (Figure 2a), consistent with covalent bond formation. However, one alternative explanation is the slow accumulation of a product that can instead serve as an inhibitor.[29] For example, hydrolysis of **1** can yield a hydroxamic acid (**3**), which is a common metal-binding pharmacophore that could possibly inactivate NDM-1 by metal ion removal.[30] We tested for inactivation by the accumulating product by inactivating NDM-1 and then adding a second, fresh aliquot of uninhibited NDM-1 to the same preincubation solution. If the accumulating product was responsible for inhibition, faster inactivation rates are expected after the second aliquot. However, the observed inactivation rate after the second addition of NDM-1 (0.007 ± 0.001 min^{-1}) was lower than after the first addition (0.012 ± 0.001 min^{-1}) and is therefore inconsistent with the proposal of an accumulating product being the inactivating species (Figure 2b).

A few different types of covalent inhibitors for NDM-1 have previously been reported, and these inactivators target either Cys208, which serves as a ligand for zinc-2, or Lys211, which helps to bind the carboxylic acid found in most β-lactam substrates.[14,17,31−33] We previously reported and characterized NDM-1 mutants at each of these sites: C208D, which removes all Cys residues from our soluble NDM-1 construct yet still supports zinc-2 binding, and K211A, which removes only one of eight total Lys residues, all of which, except for Lys125, are solvent accessible.[17] Each of these two mutant NDM-1 enzymes (C208D and K211A) retains β-lactamase activity, so we tested each to see if a change in either side chain could prevent time-dependent inactivation by **1**. The C208D mutation of NDM-1 can still be inactivated by **1**, suggesting that Cys208 is not targeted for covalent modification or is otherwise essential for inactivation (Figure 2c). In contrast, the K211A mutation of NDM-1 prevents inactivation by **1**, indicating that either Lys211 is a nucleophile targeted for covalent modification and thereby enzyme inactivation or Lys211 is otherwise essential for **1** to bind or react (Figure 2d).

Because **1** and similar compounds are known to readily undergo hydrolysis,[5] we sought to determine the rate constant for non-enzymatic hydrolysis under the same experimental conditions used for enzyme inactivation by quantifying the time-dependent release of phenol (Figure 3b,c). We also measured the time and concentration dependence of **1** inactivation of NDM-1 (Figure 3a,c). Under these conditions, the magnitude of the rate constant for non-enzymatic

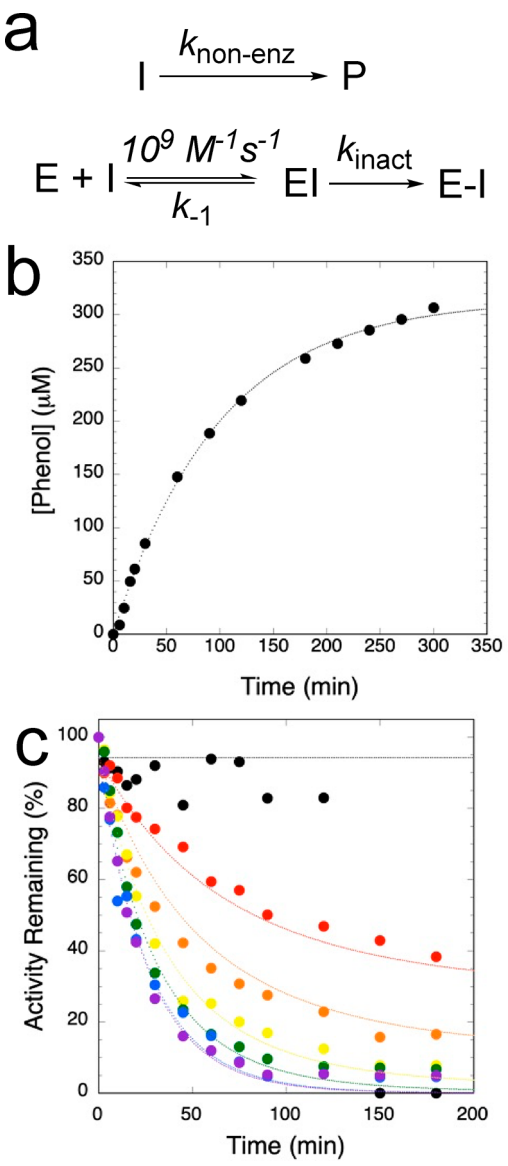

Figure 3. Global kinetic fitting. (a) Kinetic mechanism used to model non-enzymatic hydrolysis of **1** (top) and affinity labeling of NDM-1 (below). (b) Non-enzymatic hydrolysis of **1** (0.4 mM) was monitored by determining time-dependent production of phenol. (c) Time- and concentration-dependent inactivation of NDM-1 was monitored by a dilution assay (see Experimental Procedures), using 0 (black), 50 (red), 100 (orange), 250 (yellow), 500 (green), 1000 (blue), and 2000 (purple) μM **1**. Kintek Global Kinetic Explorer was used to determine global fits of data in panels b and c, and the fits are shown as dotted lines of the corresponding color.

DOI: 10.1021/acs.biochem.9b00393
Biochemistry XXXX, XXX, XXX−XXX

hydrolysis of **1** is similar to that for NDM-1 inactivation (see below). Therefore, we did not use a Kitz−Wilson analysis or Tsou plot to determine inactivation parameters because the concentration of the inactivator would not remain constant over the incubation time but instead used a global simulation method to simultaneously fit both **1** hydrolysis and NDM-1 inactivation kinetics using the minimal kinetic mechanism shown in Figure 3a.[18,19,34,35] This mechanism proposes a one-step non-enzymatic hydrolysis of **1** to release phenol and a two-step inactivation mechanism for NDM-1 that proceeds through rapid formation of an initial reversible noncovalent complex followed by an irreversible inactivation step. Using these assumptions, fits to the experimental data (Figure 3b,c) gave values for k_{nonenz} (0.010 ± 0.001 min^{-1}), k_{-1} [(8.6 ± 0.7) × 10^6 min^{-1}], and k_{inact} (0.045 ± 0.004 min^{-1}), which enabled the further calculation of K_I (140 ± 10 μM) and k_{inact}/K_I (5.4 ± 0.9 M^{-1} s^{-1}). Use of a two-step model for enzyme inactivation that includes an initial noncovalent binding step is necessary to achieve good fits. For inactivation of serine-β-lactamases, the addition of an enzyme-catalyzed partitioning step (from the noncovalent EI complex) to form a non-inhibitory product is required to achieve good fits.[5] Addition of a similar partitioning step to the kinetic mechanism for NDM-1 inactivation can also be accommodated but does not greatly improve the fits and so is not included in our proposed minimal kinetic mechanism (not shown). The second-order inactivation rate constant (k_{inact}/K_I) of **1** for NDM-1 is approximately 1000-fold smaller than that for the serine-β-lactamase P99 (6100 M^{-1} s^{-1})[6] and approximately 2 × 10^6-fold larger than that for reaction with water (estimated by k_{nonenz}/55.5 M water). Taken together, these results are consistent with the proposal that **1** is a classical affinity label with moderate potency for NDM-1.

Mass Spectrometry. To confirm and characterize covalent labeling, we used mass spectrometry to compare NDM-1 before and after incubation with **1**. To determine the mass addition and stoichiometry of any covalent adduct(s), we first used ESI-MS to characterize intact protein. The deconvoluted mass spectra for intact NDM-1 before inactivation indicate a monoisotopic mass (24823.29 Da) that is increased by 193.11 Da in samples that have been incubated with excess **1** (25016.40 Da) (Figure 4). A very minor species is also observed at 25209.41 Da, indicating the presence of a small amount of double labeling by this ∼193 Da covalent adduct. To determine which particular amino acid is covalently modified, we further characterized the **1**-treated NDM-1 protein by using UVPD fragmentation of the precursor (+28 charge state) to obtain a very extensive sequence map (Figure 5), wherein backbone cleavages occur between nearly every pair of amino acids. This UVPD sequence map provides unambiguous identification of the major covalent modification site of **1** as residue Lys211 and also confirms the amino acid sequence of NDM-1 that is encoded by the bla_{NDM} gene of our expression vector. The covalent +193.11 Da adduct matches very accurately the mass of the predicted adduct formed by attack of Lys211 on the carbonate carbon of **1**, followed by loss of phenol and an additional proton from the attacking Lys residue [193.04 Da (see below)]. These results support the proposal that **1** inactivates NDM-1 specifically by a single covalent modification of a Lys residue found at the active site of this enzyme.

Structural Determination. To obtain more information about how affinity label **1** binds and reacts with NDM-1, we determined an X-ray crystal structure of the inactivated complex to 2.0 Å resolution (Table 1). Although soluble constructs of NDM-1 are active as monomers in solution,[4,13,23,36] NDM is commonly observed to engage in homo-oligomeric interactions in crystals, often making interactions through a β-hairpin loop (Tyr64−Ala74) that is used to bind substrates.[37] Here, the individual NDM-1 monomers are found to have an overall fold and dinuclear zinc-site structure that can be closely superimposed with that of previously reported NDM-1 structures (not shown). A crystallographic dimer is again observed, formed in part through an intertwining of the substrate-binding β-hairpin loops of neighboring monomers (Figure 6a,b). These same loops also interact with the bound affinity label, although the interaction is not symmetrical. The exact positioning of the loop and the structures of the bound ligands differ between the intertwined monomers, with notable differences described below.

Extra electron density is observed in each active site that is not fit by the protein's amino acids, zinc ions, components used to promote crystallography (e.g., PEG), or water molecules (Figure 6b−d). In one monomer (chain A), the extra density is fit well by a covalent adduct attached to the ε-amino group of Lys211, with a proposed structure matching that expected to form upon attack of the carbonate carbon of **1** by the Lys211 side chain and subsequent loss of phenol [the +193 Da adduct (see below)]. This result confirms the selective covalent modification of Lys211 detected by MS and provides additional details about the conformation that the

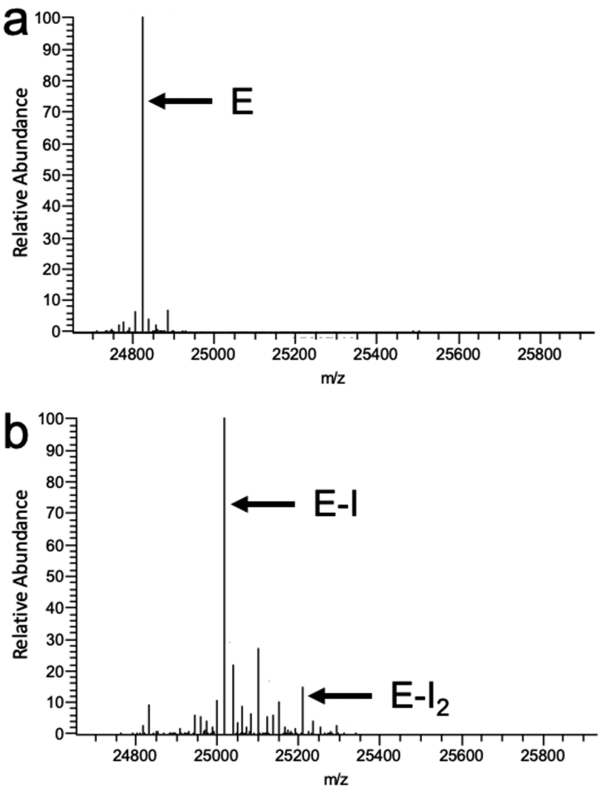

Figure 4. Deconvoluted mass spectra of intact NDM-1 before and after inactivation by **1**. (a) NDM-1 before inactivation showing the dominant species marked by E at 24823.29 Da. (b) NDM-1 after inactivation, revealing a major species marked by E-I at 25016.40 Da, which indicates an adduct of 193.11 Da. A minor species is also observed, marked by E-I_2 at 25209.41 Da, and is discussed in the text.

DOI: 10.1021/acs.biochem.9b00393
Biochemistry XXXX, XXX, XXX−XXX

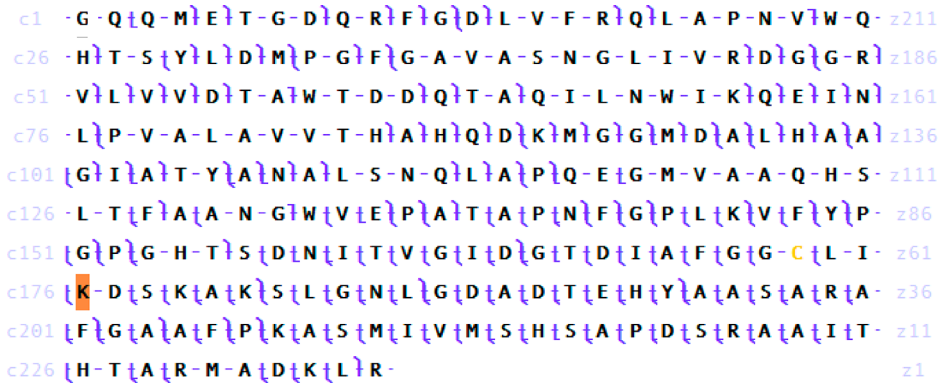

Figure 5. Sequence map of the covalent adduct to Lys211. Identified fragments from UVPD fragmentation of the +28 species of **1**-treated NDM-1 using one pulse at 2.0 mJ. One thousand scans were averaged at 240000 resolution at m/z 400. A 10 ppm mass accuracy constraint was used for fragment identification. The P score was 8.45×10^{-142}. The highlighted K indicates the amino acid site of mass addition after reaction with **1** (+193.04 Da). Cys208 (unmodified) is colored yellow.

Table 1. Crystallographic Data of 1-treated NDM-1

space group	$P2_12_12_1$
cell constants (Å)	a = 39.0, b = 73.9, c = 145.6
resolution (Å) (outer shell)	50−2.02 (2.05−2.02)
R_{merge} (%) (outer shell)	0.126 (0.545)
$\langle I/\sigma_I \rangle$ (outer shell)	5.7 (2.3)
completeness (%) (outer shell)	99.8 (98.1)
no. of unique reflections	28507
redundancy	7.0 (5.6)
no. of residues	454
no. of protein atoms	3320
no. of ligand atoms	29
no. of solvent atoms	221
no. of metal atoms	8
$R_{working}$	0.183
R_{free}	0.231
average B factor for protein atoms (Å^2)	18.8
average B factor for ligand atoms (Å^2)	35.9
average B factor for solvent atoms (Å^2)	21.3
average B factor for metal atoms (Å^2)	27.4
root-mean-square deviation from ideality	
bonds (Å)	0.006
angles (deg)	0.81
Ramachandran plot	
% of residues in most favored regions	98.0
% of residues in additional allowed regions	2.0

covalent adduct adopts after inactivation. In the second monomer (chain B), the extra electron density is better fit by two ligands, a covalent N^{ϵ}-carbamylation of Lys211 (now repositioned) and a noncovalently bound hydroxamic acid. The stabilization of a carbamylated Lys by H-bonding instead of metal ion coordination has precedence in the case of the class D serine-β-lactamase OXA10.[38] In the NDM-1 complex described here, the Lys211 carbamylation modification may be analogously stabilized through H-bonding to the water molecule ligated to zinc-2 and the backbone carbonyl oxygen of Cys208. The two ligands observed in chain B can be formed by hydrolysis of a precursor adduct that matches the structure of the single +193 Da adduct observed in chain A. Because the MS analysis did not indicate a significant +43 Da product (for Lys carbamylation) and because the noncovalently bound hydroxamate product is not coordinated to the active-site zinc cluster, it is likely that the two separate ligands observed in chain B are formed by degradation of a single +193 Da adduct during or following crystallization rather than through independent binding mechanisms.

In contrast to the differences in covalent ligand attachments, the phenyl ring of each **1**-derived ligand is bound in a similar manner by each monomer (Abstract Graphic). Key interactions in both monomers include packing the face of the phenyl ring against the side chain of Val73, which forms part of a conserved hydrophobic patch found in the substrate-binding β-hairpin loop. For chain A, the Phe70 side chain found at the apex of the same loop closes over the inactivator and makes an edge-to-face interaction with the inactivator's phenyl ring. Another Phe70 from the β-hairpin loop of the neighboring monomer adds a third hydrophobic surface (a tilted edge-to-face orientation) forming a pocket akin to a "C-clamp" that binds the ligand's phenyl ring. In chain B, Phe70 of the hairpin loop is more distant and does not make a direct interaction. Rather, Phe70 of the neighboring monomer's β-hairpin loop and the adjacent C^{α} atom of Gly69 complete the "C-clamp". When compared to the structure of NDM-1 bound to hydrolyzed benzylpenicillin (PDB entry 4EYF),[39] the phenyl ring of the **1**-derived adduct does not bind in the same pocket as the benzyl substituent of benzylpenicillin but is instead positioned closer to the binding site for the thiazolidine ring of the β-lactam. Also unlike previously described product-bound NDM-1 structures (e.g., ref 39), the adducts formed from **1** are not observed to make any direct coordination to the dinuclear zinc active site.

Although determination of the crystal structure of **1**-treated NDM-1 reveals specific binding interactions made with the resulting covalent adduct and its hydrolysis products, this experiment has some limitations. Some of the observed binding interactions may be the same as those formed in the initial noncovalent binding complex of **1** and NDM-1, but others may be formed only after inactivation occurs. Conversely, some binding conformations leading up to inactivation may be lost after phenol release and would not be visualized in the structure. Additionally, interactions with the neighboring β-hairpin loop are likely a result of crystallization because NDM-1 can function as a monomer in solution,[4,13,23,36] and the intertwining of these loops in the crystal may obscure interactions that could otherwise predominate in solution.

DOI: 10.1021/acs.biochem.9b00393
Biochemistry XXXX, XXX, XXX−XXX

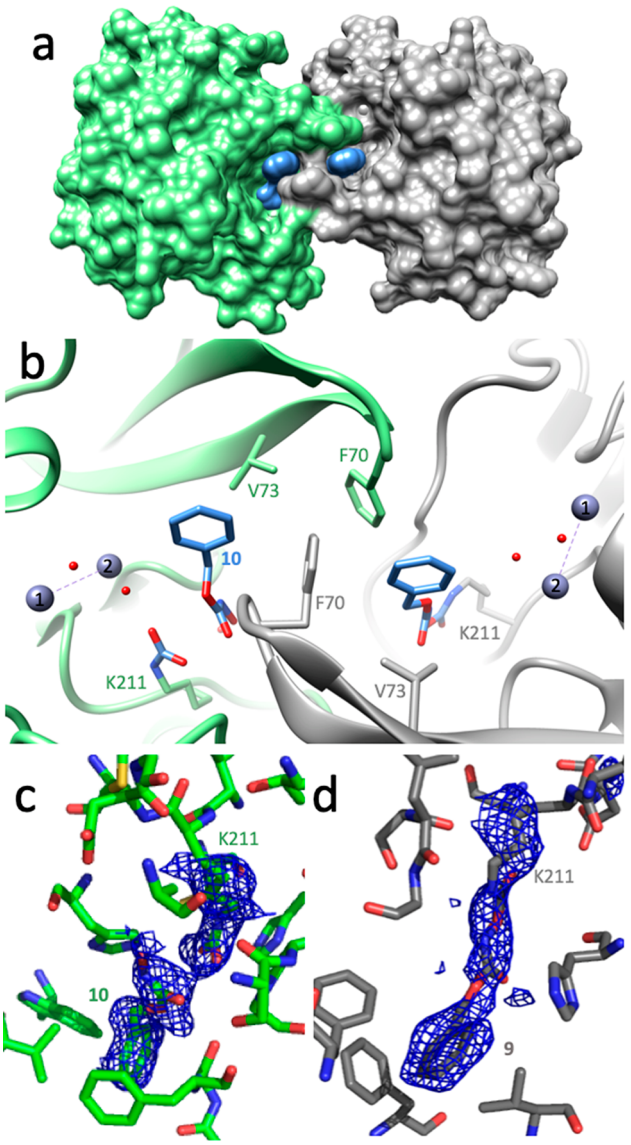

Figure 6. X-ray crystal structure of NDM-1 inactivated by **1**. (a) Surface-coated representation of the crystallographic dimer interface of NDM-1 with one monomer colored green, the other colored gray, and the inactivator colored blue. (b) Ribbon representation of the crystallographic dimer interface and active sites of each monomer, with selected residues shown as sticks and waters (red) and zinc ions (blue gray) shown as spheres. The F70 residues of the β-hairpin substrate-binding loops are intertwined. Chain A (gray) shows covalent bonding of the inactivator (colored blue and by heteroatom) to K211 as the 193 Da adduct (Figure 7, **9**), and chain B (green) shows the hydrolysis product of a noncovalently bound hydroxamic acid fragment (Figure 7, **10**) and a carbamylated K211 within H-bonding distance of a water molecule coordinated to zinc-2 (zinc-1 is labeled with a 2; zinc-1 is labeled with a 1). $F_o - F_c$ electron density maps calculated using models that omit either the side chain of N^{ϵ}-carbamylated K211 and the noncovalent product **10** (c) or the side chain of K211 with the covalent adduct **9** (d) are colored blue, contoured at 2σ.

Proposed Mechanism of Inactivation. By combining the results described above, we can propose a mechanism for NDM-1 inactivation by **1** (Figure 7) and can classify **1** as a classical affinity label for this protein.[40] Fits to a minimal kinetic mechanism are consistent with formation of an initial reversible binding complex (K_I = 140 μM), which provides selectivity for modification and fulfills one of the criteria for classical affinity labeling. Because crystallography reports on only the structure after inactivation, the conformation of the initial binding complex is undefined, and several possibilities could be considered. The phenyl ring might mimic the bicyclic rings of β-lactam substrates and bind at the hydrophobic base of the substrate-binding β-hairpin loop, inducing closure of Phe70 at the apex of this loop. The carbamate carbonyl might coordinate to one of the active-site zinc ions, similar to the proposed Michaelis complex for β-lactam substrates. Alternatively, the low pK_a of **1** (6.8) might allow this compound to mimic the anionic reaction intermediate of NDM-1 (**6**), although deprotonation to form the anion makes **1** more resistant to hydrolysis.[6] The design of compounds that mimic substrates, intermediates, or products has been a successful strategy for NDM-1 inhibitor development,[41] and similarities found in this *O*-aryloxycarbonyl hydroxamate may facilitate initial binding. After formation of the noncovalent complex, the side chain amine of the active-site Lys211 is proposed to attack the carbonate electrophile of **1**, which is held adjacent to this residue. The resulting high effective concentration (rather than a depressed Lys pK_a) likely drives the reaction, leading to loss of phenol, formation of the +193 Da adduct (**9**), and adoption of the conformation observed in chain A. The lower k_{inact}/K_I values of NDM-1 may represent the poorer nucleophilicity of Lys211, particularly at pH 7, when compared to that of the active-site Ser of P99 β-lactamase.[6] Further degradation of the adduct during crystallography can form the N^{ϵ}-carbamylated Lys211 and hydroxamic acid **10**. The irreversible covalent modification of Lys211 (**9**) blocks substrate binding and results in the observed NDM-1 inactivation. Therefore, we find that the *O*-aryloxycarbonyl hydroxamate **1** can specifically and covalently label functionally analogous Lys residues found in both serine- and metallo-β-lactamases but that labeling of NDM-1 occurs through a direct attack of Lys on bound **1**, whereas labeling of P99 β-lactamase occurs by Lys attack of a preceding covalent adduct formed at the active-site Ser (Figures 1a and 7).[6]

CONCLUSIONS

Although serine- and metallo-β-lactamases differ drastically in sequence, protein fold, and catalytic mechanism, these differences might be bridged by common features that have emerged through convergent evolution. Here, we show that an *O*-aryloxycarbonyl hydroxamate affinity label that targets a specific Lys residue (Lys315) used for substrate binding in the serine-β-lactamase P99 can also specifically label a specific Lys residue (Lys211) in NDM-1 that serves a similar purpose. The inactivation mechanisms for these two targets differ considerably, but they each involve an attack on the same carbonyl carbon of the inactivator to result in covalent Lys modification. Previous design efforts to develop wide-spectrum β-lactamase inhibitors have also relied on the shared function of these divergent enzymes to bind β-lactams but have not previously targeted Lys for covalent modification.[42−49] This particular Lys residue is conserved in most other B1-subclass metallo-β-lactamases (e.g., NDM, IMP, CcrA, BcII, and SPM) but not in VIMs, which have a more distant Arg residue that serves an analogous function.[11,50−54] Although the instability of **1** precludes application as an antibacterial agent in its current form, this Lys-targeted affinity label can selectively modify the active sites of clinically relevant serine- and metallo-β-

DOI: 10.1021/acs.biochem.9b00393
Biochemistry XXXX, XXX, XXX−XXX

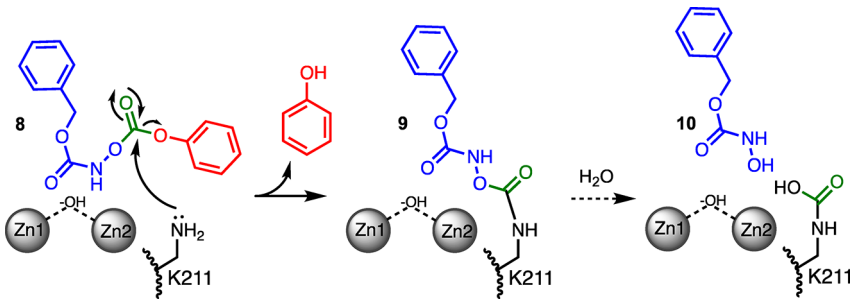

Figure 7. Proposed mechanism of affinity labeling of NDM-1 by **1**. One possible noncovalent binding complex is depicted (**8**), and others are discussed in the text. Formation of a noncovalent complex provides a high effective molarity of the electrophile, promoting nucleophilic attack by the side chain amine of Lys211 and loss of phenol. The resulting +193 Da adduct (**9**) results in enzyme inactivation by blocking substrate binding at the active site and is irreversible to dilution in excess substrate. During crystallography, **9** can degrade to form an N^{ϵ}-carbamylated K211 and a noncovalently bound hydroxamic acid (**10**).

lactamases, suggesting a new strategy for the development of covalent, wide-spectrum β-lactamase inhibitors.

■ ASSOCIATED CONTENT

Accession Codes

Uniprot: NDM-1, C7C422. NCBI Protein: NDM-1, ARK36277. Protein Data Bank: NDM-1 inactivated by **1**, 6OVZ.

■ AUTHOR INFORMATION

Corresponding Authors

*E-mail: walt.fast@austin.utexas.edu.

*E-mail: rpratt@wesleyan.edu.

ORCID

Jennifer S. Brodbelt: 0000-0003-3207-0217

R. F. Pratt: 0000-0002-1381-2556

Walter Fast: 0000-0001-7567-2213

Funding

This work was supported in part by the National Institutes of Health (Grant GM111926 to W.F.), the National Science Foundation (Grant CHE-1402753 to J.S.B.), and the Robert A. Welch Foundation (Grants F-1572 to W.F. and F-1155 to J.S.B.).

Notes

The authors declare no competing financial interest.

■ ACKNOWLEDGMENTS

The authors thank Ken Johnson (The University of Texas at Austin) for the generous gift of the KinTek Explorer software package. Assistance was provided by the Macromolecular Crystallography Facility, with financial support from the College of Natural Sciences, the Office of the Executive Vice President and Provost, and the Institute for Cellular and Molecular Biology at The University of Texas at Austin. The Berkeley Center for Structural Biology is supported in part by the National Institutes of Health, National Institute of General Medical Sciences, and the Howard Hughes Medical Institute. The Advanced Light Source is supported by the Director, Office of Science, Office of Basic Energy Sciences, of the U.S. Department of Energy under Contract DE-AC02-05CH11231.

■ REFERENCES

(1) Drawz, S. M., and Bonomo, R. A. (2010) Three decades of beta-lactamase inhibitors. *Clin. Microbiol. Rev. 23*, 160−201.

(2) Ehmann, D. E., Jahic, H., Ross, P. L., Gu, R. F., Hu, J., Kern, G., Walkup, G. K., and Fisher, S. L. (2012) Avibactam is a covalent, reversible, non-beta-lactam beta-lactamase inhibitor. *Proc. Natl. Acad. Sci. U. S. A. 109*, 11663−11668.

(3) Lohans, C. T., Brem, J., and Schofield, C. J. (2017) New Delhi Metallo-beta-Lactamase 1 Catalyzes Avibactam and Aztreonam Hydrolysis. *Antimicrob. Agents Chemother. 61*, e01224-17.

(4) Yang, H., Aitha, M., Hetrick, A. M., Richmond, T. K., Tierney, D. L., and Crowder, M. W. (2012) Mechanistic and spectroscopic studies of metallo-beta-lactamase NDM-1. *Biochemistry 51*, 3839−3847.

(5) Wyrembak, P. N., Babaoglu, K., Pelto, R. B., Shoichet, B. K., and Pratt, R. F. (2007) O-aryloxycarbonyl hydroxamates: new beta-lactamase inhibitors that cross-link the active site. *J. Am. Chem. Soc. 129*, 9548−9549.

(6) Pelto, R. B., and Pratt, R. F. (2008) Kinetics and mechanism of inhibition of a serine beta-lactamase by *O*-aryloxycarbonyl hydroxamates. *Biochemistry 47*, 12037−12046.

(7) Tilvawala, R., and Pratt, R. F. (2013) Covalent inhibition of serine beta-lactamases by novel hydroxamic acid derivatives. *Biochemistry 52*, 3712−3720.

(8) Tilvawala, R., Cammarata, M., Adediran, S. A., Brodbelt, J. S., and Pratt, R. F. (2015) A New Covalent Inhibitor of Class C beta-Lactamases Reveals Extended Active Site Specificity. *Biochemistry 54*, 7375−7384.

(9) Malico, A. A., Dave, K., Adediran, S. A., and Pratt, R. F. (2019) Specificity of extended *O*-aryloxycarbonyl hydroxamates as inhibitors of a class C beta-lactamase. *Bioorg. Med. Chem. 27*, 1430−1436.

(10) Lobkovsky, E., Moews, P. C., Liu, H., Zhao, H., Frere, J. M., and Knox, J. R. (1993) Evolution of an enzyme activity: crystallographic structure at 2-Å resolution of cephalosporinase from the ampC gene of *Enterobacter cloacae* P99 and comparison with a class A penicillinase. *Proc. Natl. Acad. Sci. U. S. A. 90*, 11257−11261.

(11) Zhang, H., and Hao, Q. (2011) Crystal structure of NDM-1 reveals a common beta-lactam hydrolysis mechanism. *FASEB J. 25*, 2574−2582.

(12) Adediran, S. A., and Pratt, R. F. (2017) Penicillin acylase and *O*-aryloxycarbonyl hydroxamates: Two acyl-enzymes, one leading to hydrolysis, the other to inactivation. *Arch. Biochem. Biophys. 614*, 65−71.

(13) Thomas, P. W., Zheng, M., Wu, S., Guo, H., Liu, D., Xu, D., and Fast, W. (2011) Characterization of purified New Delhi metallo-beta-lactamase-1. *Biochemistry 50*, 10102−10113.

(14) Thomas, P. W., Cammarata, M., Brodbelt, J. S., and Fast, W. (2014) Covalent inhibition of New Delhi metallo-beta-lactamase-1 (NDM-1) by cefaclor. *ChemBioChem 15*, 2541−2548.

(15) Yu, S., Vosbeek, A., Corbella, K., Severson, J., Schesser, J., and Sutton, L. D. (2012) A chromogenic cephalosporin for beta-lactamase inhibitor screening assays. *Anal. Biochem. 428*, 96−98.

(16) Chen, A. Y., Thomas, P. W., Stewart, A. C., Bergstrom, A., Cheng, Z., Miller, C., Bethel, C. R., Marshall, S. H., Credille, C. V.,

DOI: 10.1021/acs.biochem.9b00393
Biochemistry XXXX, XXX, XXX−XXX

Riley, C. L., Page, R. C., Bonomo, R. A., Crowder, M. W., Tierney, D. L., Fast, W., and Cohen, S. M. (2017) Dipicolinic Acid Derivatives as Inhibitors of New Delhi Metallo-beta-lactamase-1. *J. Med. Chem. 60*, 7267−7283.

(17) Thomas, P. W., Spicer, T., Cammarata, M., Brodbelt, J. S., Hodder, P., and Fast, W. (2013) An altered zinc-binding site confers resistance to a covalent inactivator of New Delhi metallo-beta-lactamase-1 (NDM-1) discovered by high-throughput screening. *Bioorg. Med. Chem. 21*, 3138−3146.

(18) Johnson, K. A. (2009) Fitting enzyme kinetic data with KinTek Global Kinetic Explorer. *Methods Enzymol. 467*, 601−626.

(19) Johnson, K. A., Simpson, Z. B., and Blom, T. (2009) Global kinetic explorer: a new computer program for dynamic simulation and fitting of kinetic data. *Anal. Biochem. 387*, 20−29.

(20) Han, S. W., Lee, S. W., Bahar, O., Schwessinger, B., Robinson, M. R., Shaw, J. B., Madsen, J. A., Brodbelt, J. S., and Ronald, P. C. (2012) Tyrosine sulfation in a Gram-negative bacterium. *Nat. Commun. 3*, 1153.

(21) Otwinowski, Z., and Minor, W. (1997) Processing of X-ray diffraction data collected in oscillation mode. *Methods Enzymol. 276*, 307−326.

(22) McCoy, A. J., Grosse-Kunstleve, R. W., Adams, P. D., Winn, M. D., Storoni, L. C., and Read, R. J. (2007) Phaser crystallographic software. *J. Appl. Crystallogr. 40*, 658−674.

(23) Guo, Y., Wang, J., Niu, G., Shui, W., Sun, Y., Zhou, H., Zhang, Y., Yang, C., Lou, Z., and Rao, Z. (2011) A structural view of the antibiotic degradation enzyme NDM-1 from a superbug. *Protein Cell 2*, 384−394.

(24) Emsley, P., Lohkamp, B., Scott, W. G., and Cowtan, K. (2010) Features and development of Coot. *Acta Crystallogr., Sect. D: Biol. Crystallogr. 66*, 486−501.

(25) Adams, P. D., Afonine, P. V., Bunkoczi, G., Chen, V. B., Davis, I. W., Echols, N., Headd, J. J., Hung, L. W., Kapral, G. J., Grosse-Kunstleve, R. W., McCoy, A. J., Moriarty, N. W., Oeffner, R., Read, R. J., Richardson, D. C., Richardson, J. S., Terwilliger, T. C., and Zwart, P. H. (2010) PHENIX: a comprehensive Python-based system for macromolecular structure solution. *Acta Crystallogr., Sect. D: Biol. Crystallogr. 66*, 213−221.

(26) Read, R. J. (1986) Improved Fourier Coefficients for Maps Using Phases from Partial Structures with Errors. *Acta Crystallogr., Sect. A: Found. Crystallogr. 42*, 140−149.

(27) Brunger, A. T. (1993) Assessment of phase accuracy by cross validation: the free R value. Methods and applications. *Acta Crystallogr., Sect. D: Biol. Crystallogr. 49*, 24−36.

(28) Davis, I. W., Leaver-Fay, A., Chen, V. B., Block, J. N., Kapral, G. J., Wang, X., Murray, L. W., Arendall, W. B., 3rd, Snoeyink, J., Richardson, J. S., and Richardson, D. C. (2007) MolProbity: all-atom contacts and structure validation for proteins and nucleic acids. *Nucleic Acids Res. 35*, W375−383.

(29) Silverman, R. B. (1995) Mechanism-based enzyme inactivators. *Methods Enzymol. 249*, 240−283.

(30) Kawai, K., and Nagata, N. (2012) Metal-ligand interactions: an analysis of zinc binding groups using the Protein Data Bank. *Eur. J. Med. Chem. 51*, 271−276.

(31) Chiou, J., Wan, S., Chan, K. F., So, P. K., He, D., Chan, E. W., Chan, T. H., Wong, K. Y., Tao, J., and Chen, S. (2015) Ebselen as a potent covalent inhibitor of New Delhi metallo-beta-lactamase (NDM-1). *Chem. Commun. 51*, 9543−9546.

(32) Christopeit, T., Albert, A., and Leiros, H. S. (2016) Discovery of a novel covalent non-beta-lactam inhibitor of the metallo-beta-lactamase NDM-1. *Bioorg. Med. Chem. 24*, 2947−2953.

(33) Su, J., Liu, J., Chen, C., Zhang, Y., and Yang, K. (2019) Ebsulfur as a potent scaffold for inhibition and labelling of New Delhi metallo-beta-lactamase-1 in vitro and in vivo. *Bioorg. Chem. 84*, 192−201.

(34) Kitz, R., and Wilson, I. B. (1962) Esters of methanesulfonic acid as irreversible inhibitors of acetylcholinesterase. *J. Biol. Chem. 237*, 3245−3249.

(35) Tsou, C. L. (2006) Kinetics of substrate reaction during irreversible modification of enzyme activity. *Adv. Enzymol. Relat. Areas Mol. Biol. 61*, 381−436.

(36) Yong, D., Toleman, M. A., Giske, C. G., Cho, H. S., Sundman, K., Lee, K., and Walsh, T. R. (2009) Characterization of a new metallo-beta-lactamase gene, bla(NDM-1), and a novel erythromycin esterase gene carried on a unique genetic structure in *Klebsiella pneumoniae* sequence type 14 from India. *Antimicrob. Agents Chemother. 53*, 5046−5054.

(37) Fast, W., and Sutton, L. D. (2013) Metallo-beta-lactamase: inhibitors and reporter substrates. *Biochim. Biophys. Acta, Proteins Proteomics 1834*, 1648−1659.

(38) Maveyraud, L., Golemi, D., Kotra, L. P., Tranier, S., Vakulenko, S., Mobashery, S., and Samama, J. P. (2000) Insights into class D beta-lactamases are revealed by the crystal structure of the OXA10 enzyme from *Pseudomonas aeruginosa*. *Structure 8*, 1289−1298.

(39) King, D. T., Worrall, L. J., Gruninger, R., and Strynadka, N. C. (2012) New Delhi metallo-beta-lactamase: structural insights into beta-lactam recognition and inhibition. *J. Am. Chem. Soc. 134*, 11362−11365.

(40) Tuley, A., and Fast, W. (2018) The Taxonomy of Covalent Inhibitors. *Biochemistry 57*, 3326−3337.

(41) Ju, L. C., Cheng, Z., Fast, W., Bonomo, R. A., and Crowder, M. W. (2018) The Continuing Challenge of Metallo-beta-Lactamase Inhibition: Mechanism Matters. *Trends Pharmacol. Sci. 39*, 635−647.

(42) Bush, K., Macalintal, C., Rasmussen, B. A., Lee, V. J., and Yang, Y. (1993) Kinetic interactions of tazobactam with beta-lactamases from all major structural classes. *Antimicrob. Agents Chemother. 37*, 851−858.

(43) Nagano, R., Adachi, Y., Imamura, H., Yamada, K., Hashizume, T., and Morishima, H. (1999) Carbapenem derivatives as potential inhibitors of various beta-lactamases, including class B metallo-beta-lactamases. *Antimicrob. Agents Chemother. 43*, 2497−2503.

(44) Buynak, J. D., Chen, H., Vogeti, L., Gadhachanda, V. R., Buchanan, C. A., Palzkill, T., Shaw, R. W., Spencer, J., and Walsh, T. R. (2004) Penicillin-derived inhibitors that simultaneously target both metallo- and serine-beta-lactamases. *Bioorg. Med. Chem. Lett. 14*, 1299−1304.

(45) Venkatesan, A. M., Agarwal, A., Abe, T., Ushirogochi, H., Yamamura, I., Kumagai, T., Petersen, P. J., Weiss, W. J., Lenoy, E., Yang, Y., Shlaes, D. M., Ryan, J. L., and Mansour, T. S. (2004) Novel imidazole substituted 6-methylidene-penems as broad-spectrum beta-lactamase inhibitors. *Bioorg. Med. Chem. 12*, 5807−5817.

(46) Ganta, S. R., Perumal, S., Pagadala, S. R., Samuelsen, O., Spencer, J., Pratt, R. F., and Buynak, J. D. (2009) Approaches to the simultaneous inactivation of metallo- and serine-beta-lactamases. *Bioorg. Med. Chem. Lett. 19*, 1618−1622.

(47) Johnson, J. W., Gretes, M., Goodfellow, V. J., Marrone, L., Heynen, M. L., Strynadka, N. C., and Dmitrienko, G. I. (2010) Cyclobutanone analogues of beta-lactams revisited: insights into conformational requirements for inhibition of serine- and metallo-beta-lactamases. *J. Am. Chem. Soc. 132*, 2558−2560.

(48) Brem, J., Cain, R., Cahill, S., McDonough, M. A., Clifton, I. J., Jimenez-Castellanos, J. C., Avison, M. B., Spencer, J., Fishwick, C. W., and Schofield, C. J. (2016) Structural basis of metallo-beta-lactamase, serine-beta-lactamase and penicillin-binding protein inhibition by cyclic boronates. *Nat. Commun. 7*, 12406.

(49) Torelli, N. J., Akhtar, A., DeFrees, K., Jaishankar, P., Pemberton, O. A., Zhang, X., Johnson, C., Renslo, A. R., and Chen, Y. (2019) Active-Site Druggability of Carbapenemases and Broad-Spectrum Inhibitor Discovery. *ACS Infect. Dis.*, DOI: 10.1021/acsinfecdis.9b00052.

(50) Concha, N. O., Janson, C. A., Rowling, P., Pearson, S., Cheever, C. A., Clarke, B. P., Lewis, C., Galleni, M., Frere, J. M., Payne, D. J., Bateson, J. H., and Abdel-Meguid, S. S. (2000) Crystal structure of the IMP-1 metallo beta-lactamase from *Pseudomonas aeruginosa* and its complex with a mercaptocarboxylate inhibitor: binding determinants of a potent, broad-spectrum inhibitor. *Biochemistry 39*, 4288−4298.

DOI: 10.1021/acs.biochem.9b00393
Biochemistry XXXX, XXX, XXX−XXX

(51) Concha, N. O., Rasmussen, B. A., Bush, K., and Herzberg, O. (1996) Crystal structure of the wide-spectrum binuclear zinc beta-lactamase from *Bacteroides fragilis*. *Structure 4*, 823−836.
(52) Carfi, A., Pares, S., Duee, E., Galleni, M., Duez, C., Frere, J. M., and Dideberg, O. (1995) The 3-D structure of a zinc metallo-beta-lactamase from *Bacillus cereus* reveals a new type of protein fold. *EMBO J. 14*, 4914−4921.
(53) Murphy, T. A., Catto, L. E., Halford, S. E., Hadfield, A. T., Minor, W., Walsh, T. R., and Spencer, J. (2006) Crystal structure of *Pseudomonas aeruginosa* SPM-1 provides insights into variable zinc affinity of metallo-beta-lactamases. *J. Mol. Biol. 357*, 890−903.
(54) Garcia-Saez, I., Docquier, J. D., Rossolini, G. M., and Dideberg, O. (2008) The three-dimensional structure of VIM-2, a Zn-beta-lactamase from *Pseudomonas aeruginosa* in its reduced and oxidised form. *J. Mol. Biol. 375*, 604−611.

DOI: 10.1021/acs.biochem.9b00393
Biochemistry XXXX, XXX, XXX−XXX